Portable small UAV

Team members: Almog Dov, Assaf Alush, Bar Ovadia, Dafna Lavi, Orad Eldar.
Supervisor: Dror Artzi

Technion – Israel Institute of Technology, Haifa, Israel

I. ABSTRACT

This project deals with small portable UAV, single-man operated and uses for over-the-hill observation.

The concept is a flying wing - for vertical takeoff and landing as for straight and level flight. The UAV is propelled using two independent propulsion systems: One for the vertical lift and one for the straight and level flight:

Final result is a flying wing, 4.5Kg weight and 1.8m wingspan, carried by 3 motors: located in holes inside the fuselage, and an additional rear motor with pusher propeller which allows flight time of 30 minutes and carrying a 99gr payload – NextVisionMicroCam-D system.

II. INTRODUCTION

An unmanned aerial vehicle (UAV) is an aircraft without a human pilot on board.
Its flight is controlled either autonomously by computers in the vehicle, or under the remote control of a pilot on the ground.

Table 1 presents the categories of UAVs divided by mass, range, flight altitude and endurance.

Category name	Mass [kg]	Range [km]	Flight Altitude [m]	Endurance [hours]
Micro	< 5	< 10	250	1
Mini	<25/30/ 150	< 10	150/250/ 300	< 2
Close Range	25 –150	10 – 30	3000	2 – 4
Medium Range	50 –250	30 – 70	3000	3 – 6
High Alt. Long Endurance	> 250	> 70	> 3000	> 6

Table 1

There is a wide variety of shapes, sizes, configurations, and characteristics of UAVs.
They are deployed predominantly for military and special operation applications, but also used in a small, yet growing number of civil applications such policing, firefighting and

nonmilitary security work such as surveillance of pipelines.
UAVs are often preferred for missions that are too "dull, dirty or dangerous" for manned aircraft.

These are the costumer specification and requirements for the project:

- o Man-portable UAV
- o Over the hill / Urban surveillance
- o Fast field deployment
- o Endurance: 30 min
- o Simple, operated by one man
- o Real time video camera
- o Quiet
- o Portable Ground Control System (PGCS)
- o Fully automated flight (including take-off and landing)

III. CONCEPT DEVELOPMENT AND PRELIMINARY DESIGN

The conceptual approach was based on analysis of the customer specifications and requirements as well as the market survey.

The requirement for a single operator resulted in a small UAV with no launcher - In order to make the UAV easy to carry. Moreover, the requirement for a simple operation by one man led to an automated flight with safe take-off and landing to prevent faults during operating. Furthermore, the costumer's request for a simple recovery rejected the option of using a parachute or an airbag. The above requirement resulted in a fully automated UAV with the ability of vertical take-off and landing. Despite this conclusion, the use of tilted rotor concept was rejected due to the complicated control system required to support it. As a result, it was decided to separate the propulsion system of level flight from the propulsion system of the vertical take-off and landing.

Another costumer's requirement was a UAV with capability to reach an out of sight target. This led to a necessity in fixed wing abilities in order to sustain a long distance flight.

All the above have formed an innovative idea as a students' project for a design of a UAV.

Figure 1

The sizing began with vertical take-off and landing capabilities, which means three motors in a triangle formation as can be seen in figure 2.
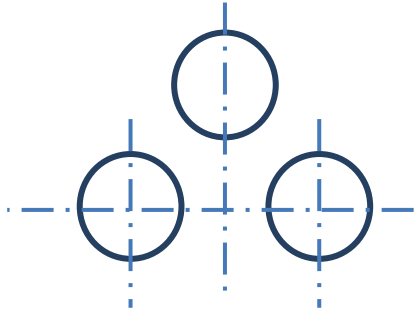
Figure 1

The configuration shown above could not fit into a fixed wing and therefore it was placed in a solid triangle (figure 3).
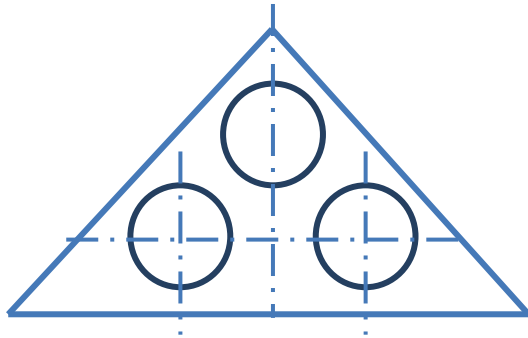

Figure2

Two outer wings were added to the configuration in order to enlarge the aspect ratio and by that to optimize the performances of the UAV (figure 4).
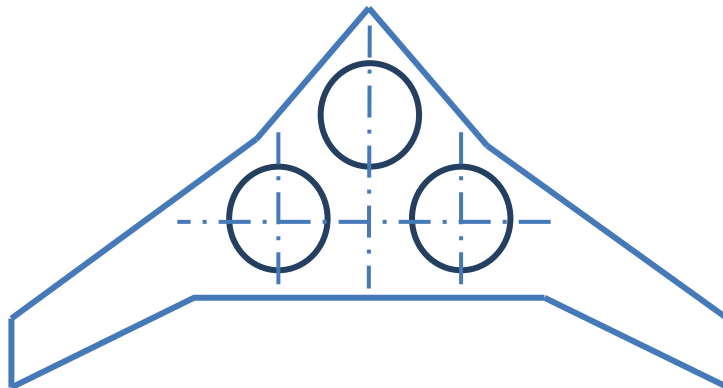

Figure 4

Component	Estimated Weight
Structure	1.1Kg
Propulsion	3.0Kg
Avionics	0.3Kg
Payload	0.1Kg
Total	**4.5Kg**

Table 2

The total weight as seen in table 4 was the first estimation of the MTOW is 4.5Kg.

In order to maintain the 4.5Kg MTOW, the structure is made of composite materials:

1. Carbon fabric for spars web and flunge, with unidirectional carbon for flange support.
2. Kevlar for the skin.

The wing structure was based on leading edge spars, trailing edge spars, ribs and mid-fuselage reinforcement (figure 5).
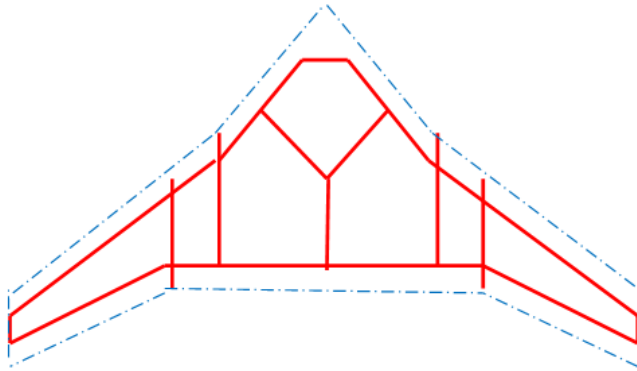

Figure 5

The lift acts as a bending force over the wing, therefore a reinforcement is needed. As accepted in aviation, this reinforcement comes as a main beam or spar along the wing.

Our wing has 2 Spars and 2 ribs: One main spar and one trailing edge spar, and tip and root ribs
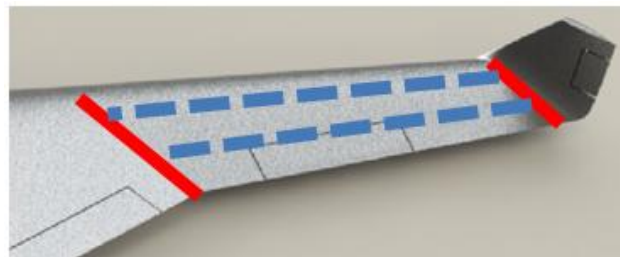

Figure 6

Figure 7

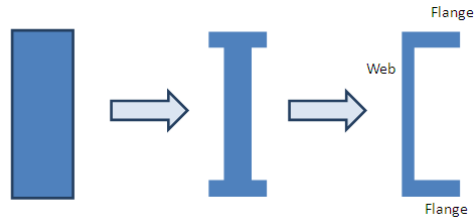Although I beam is satisfying solution, U beam can produce better performance as easier manufacturing.

Figure 8

Web and flange material: Carbon Fabric (45deg)

Flange support: Carbon unidirectional (UD)

Spar dimensions:

- ž   Main spar:

- ž

    - Web height – forced by wing geometry

    - Flange Width– Calculated by bending load analysis under the assumption of constant thickness of 1mm
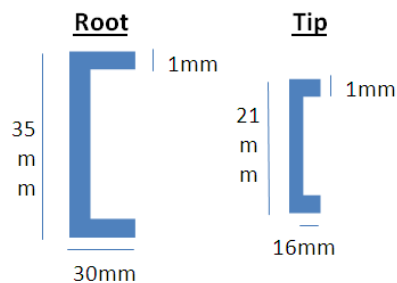

Figure 9

- ž   **Trailing edge spar:**

- ž   Web height – forced by wing geometry

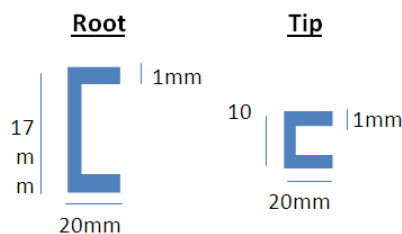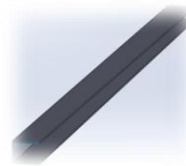- ž   Flange Width– Designed for smooth operation of the aileron control system

Figure 10

Spars location:

Main spar is located at 25% chord.
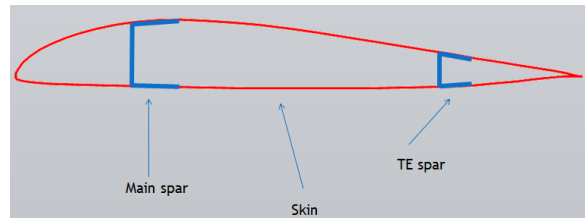Trailing edge spar is parallel to the ailerons hinges line, using for support aileron hinges.

Figure 11

Aileron control system

To minimize drag, ailerons control system is located inside the wing.
The aileron is connected to the trailing edge spar by a piano hinge at the upper surface and by control rod at the lower surface.

Movement of the aileron controlled by a servo located in the inside the wing space, attached to the trailing edge spar, as shown in the following figure.
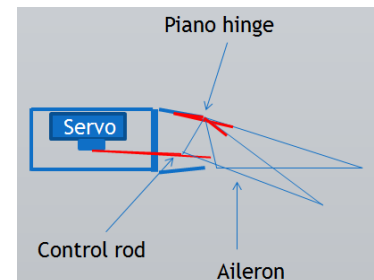
The chosen aileron servo is the Futaba S3156MG.
It has been chosen due to its high torque, low weight and high reliability.

S3156 Micro		
FUTM0656		
Volts	**Torque**	**Speed**
4.8V	28 oz-in (2.0 kg-cm)	0.13 sec/60°
6.0V	33 oz-in (2.4 kg-cm)	0.11 sec/60°
Dimensions		**Weight**
7/8 x 7/16 x 7/8 in. (22 x 11 x 22 mm)		0.33 oz (9.3 g)
		3P, BB, MG

Figure 12

Root and tip ribs

- EPPLER 334 airfoil shaped

- Tip is made of 1mm carbon fabric

  - Holes for electrical wires

  - Connection to the winglets

Figure 13

- Root is made of 3mm carbon fabric

  - Holes for electrical wires
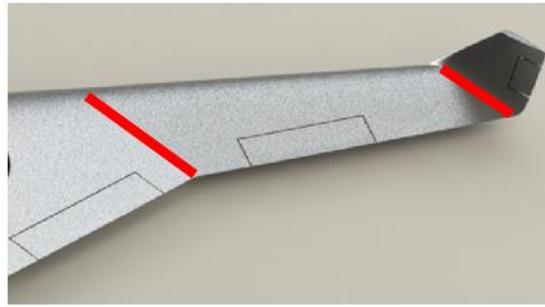
  - Supports the outer wing spars

Figure 14

Figure 15

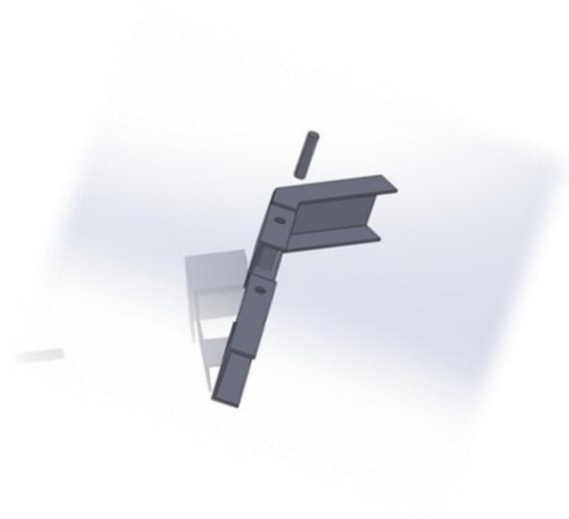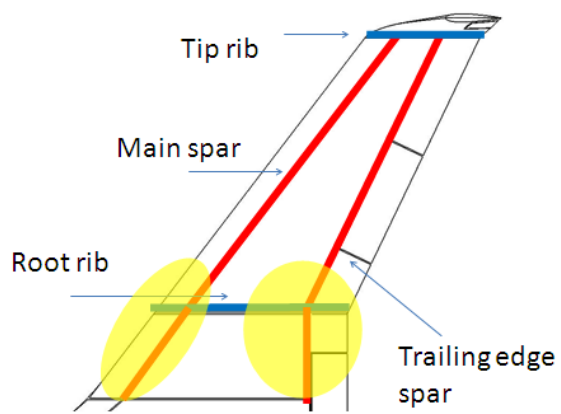Connection to the main body is made by two spars and one pin:

Figure 16 & 17

The final drawing of the UAV is shown in figure 18.
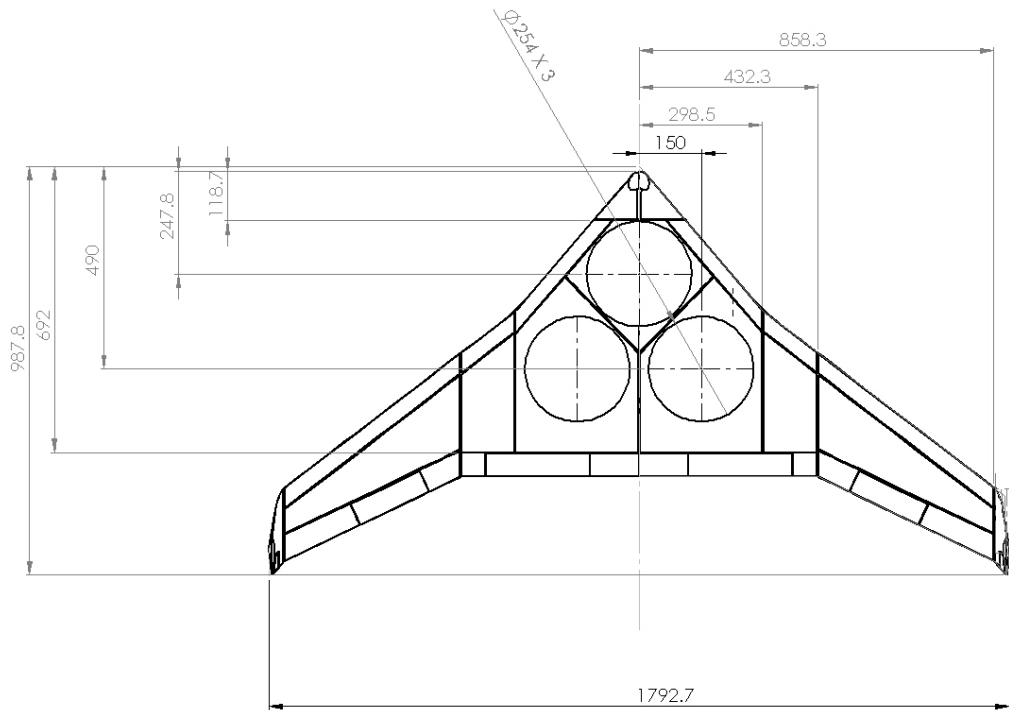
Figure 18

IV.   COMPONENTS AND SYSTEMS

MOTOR

The selection of propulsion system for vertical take-off and landing included a few decisions which followed a simple calculation based on a free body diagram (figure 19).
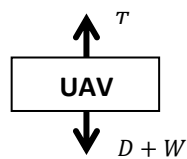
Figure 19

Where T represents the engine's thrust, D represents the drag on the UAV which is related to its surface and W represents the weight of the UAV.

To calculate the thrust each motor is required to supply, a safety factor was taken into account. Since a three motor configuration was chosen and the UAV's approximate weight is 4.5 Kg, the thrust each motor has to supply resulted in about 2.2 Kgf.

| Engine	Hacker a30-14L	OS OMA 3820-960	AXI 2820/8	AXI 2814/16	Turnigy D3536/9 910KV
Picture					
Thrust [Kgf]	2.41	2.13	2.13	2.56	1.87
Power [watt]	543	450	450	450	370
Weight [g]	143	160	151	151	102
Performance constant - Kv	800	960	860	860	910
Propeller diameter [inch]	10	10	10	10	10

Table 3

For the vertical take-off and landing, the **Hacker A30-14L** motor was chosen due to its high thrust and power, low K_V and weight.

For a 4.5 kg aircraft and cruise speed of 30 m/s (approx. 58 knots), the calculated required power was 1214 Watt. According to the drag equation, the drag at that speed is approximately 2.5Newtons.

As seen in table 4, the recommended setup according to the motor manufactures yield good results. Yet, the weight of the batteries needed to sustain a 20 minutes flight is very high. This is due to the high power required. The solution was lowering the diameter of the propeller and by that lowering the power needed. The problem with the solution proposed is the cost of flight speed.

Motor	Hacker A50 12-L	Hacker A50 14-L	AXI 4130-16
Picture			
Battery	6s	6s	6s
RPM	6440	5775	7161
Propeller	17x10	17x8	16x10
Power	1012 W	720 W	1106W
endurance	15 min	21 min	21min
Current needed	15 A	12A	18A
Total weight of motor + battery	3.3kg	2.8kg	3.8kg

Table 4

However, using 3 blades propeller with shorter diameter enables to reduce the power required to sustain fight while providing enough flight speed and thrust.

According to the motor analysis, the best motor for the aircraft is **Hacker A50 14-L**.

PROPELLER

In order to minimize the effect on the UAV's performance, the motors' holes should be as small as possible. Therefore, the minimal propeller diameter needed to provide enough power for vertical take-off and landing was found using the thrust equations above.

3 motors were used to provide total thrust of 4.5Kgf. Each is required to provide thrust of 1.5Kgf. Figure 7 shows raw calculations of thrust vs. RPM for different propeller diameters and pitch angles.
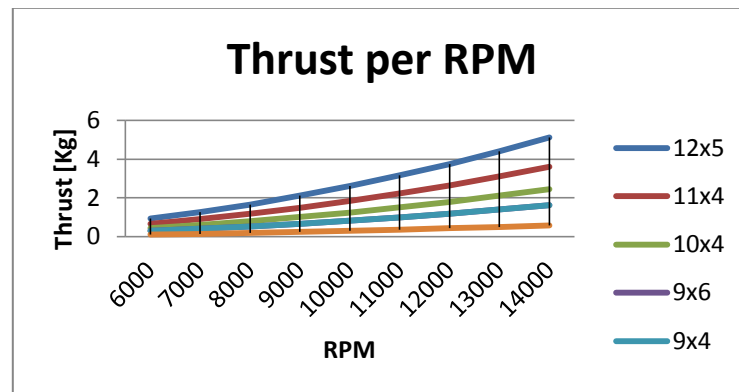

Figure 20

The reasonable RPM was deduced using the suggested motors for thrust of 1.5kgf. The RPM that was found was 10,000-11,000 and the optimal minimal diameter was 10 inches and 4 degrees pitch. Using a diameter of 9 inches may reduce the motor's holes in the body; however it may require much stronger motors which will require more power and, as a result, heavier batteries.

The calculation was based on the selected motor for level flight which had rotational speed of about 6200 RPM.

	2 blades				3 blades			
Prop size	Thrust [kg]	Req. power [W]	Total weight [kg]	Current needed [A]	Thrust [kg]	Req. power [W]	Total weight [kg]	Current needed [A]
15x8	2.64	520	2	8	3.7	728	2.1	9
15x10	2.64	650	2.1	9	3.7	911	2.7	12

Table 5

It can be seen that a 3-blade propeller provides more current that the 2-blade propeller. Therefore, we optimized the propeller size and type to a 3-blade propeller with 15 inches diameter and 8 degreespitch.

<u>BATTERIES</u>

Since an electric propulsion system was chosen, batteries are required for the motors.

For vertical take-off and landing three LiPo batteries are needed, one for each of the three Hacker motors that were chosen.

The power of each Hacker A30-14L motor: $P = 543 \, [Watt]$

The endurance requirement from the UAV: $t = \frac{4}{60} \, [Hour]$

The voltage supplied by a 4-cell LiPo battery: $V = 14.8 \, [Volt]$

The current required from each battery: $\quad I = \frac{Pt}{V} \cong 2.45 \ [A \cdot Hour]$

Battery Model	ZIPPY Compact I 300mAh 4S 35C	ZIPPY-K Flightmax 2500mAh 4S I P 20C	Thunder Power RC G6 Pro Lite 25C 2700mAh 4S	Genesis Power 4S 14.8V 2500mAh 40C
Capacity [Ah]	1.3	2.5	2.7	2.5
Weight [gr]	2x150	246	238	280
Dimensions LxWxH [mm]	78x34x29	116x33x37	102x34x34	136x44x23

Table 6

As shown in table 6, the Thunder Power battery has the highest capacity and has the lighter weight. Therefore, the Thunder Power RC G6 Pro Lite 25C 2700mAh 4S battery was chosen for vertical take-off and landing.

The power of Hacker a50-14L: $\quad P = 700 \ [Watt]$

The endurance requirement from the UAV: $\quad t = \frac{20}{60} [Hour]$

The voltage supplied by a 6-cell LiPo battery: $\quad V = 22.2 \ [Volt]$

The current required from the battery: $\ I = \frac{Pt}{V} \cong 9 \ [A \cdot Hour]$

To supply the requiredcurrent, it was decided to use two LiPo batteries, each required to supply current of $4500 \ [mA \cdot Hour]$.

Battery	Weight
Turnigy nano-tech 4500mah 6S 35~70C	676g
ZIPPY Compact 4500mAh 6S 35C	696g
Turnigy 4500mAh 6S 30C Lipo Pack	745

Table 7

The most important property is the weight of the battery, therefore the Turnigynano-tech 4500mah 6S 35~70C battery was chosen for level flight.

E/O Sensor

All sensors that were surveyed were too heavy and a compromise had to be made. Therefore, the chosen E/O sensor was the Nextvision MicroCam D. This sensor has lightweight and satisfying performance, though it is only a day sensor rather than day &night.

Model	D-STAMP	MicroPop	MicroCam D	VD/GD170
Picture				
Manufacturer	Controp	IAI	Nextvision	USA Vision
E.O Sensor	Day & Night	Day & Night	Day	Day & Night
Weight	1 Kg	700gr	99gr	900gr

Table 8

After all the systems and components were chosen, the next figure presents the installation arrangement:
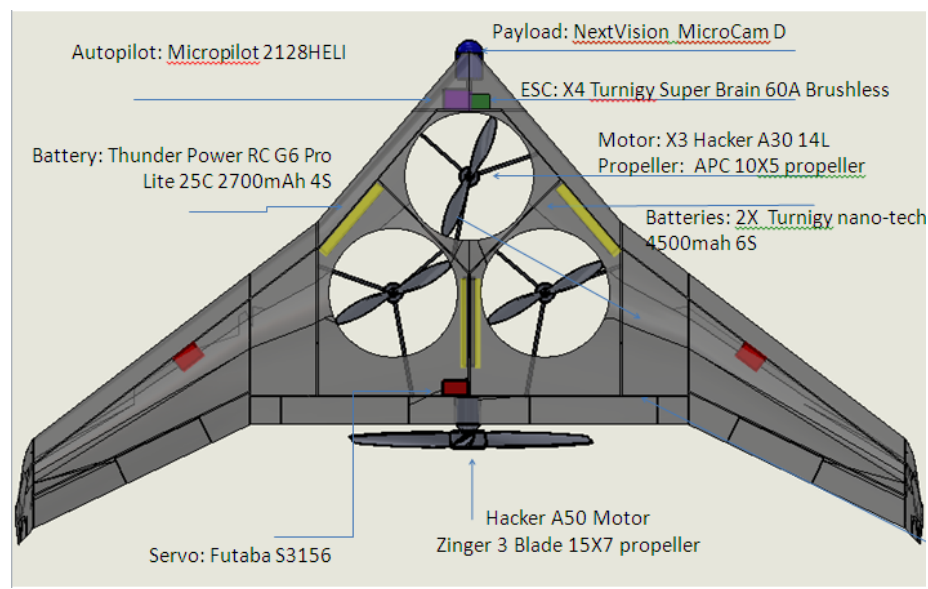

Figure 21

V. AERODYNAMICS

The configuration of flying wing has several benefits for the UAV and therefore it was chosen. First, it provides enough space for the vertical propellers, which means the UAV can take-off and land vertically. Secondly, this configuration does not require a tail so the tail can be dismissed. Since a configuration with no tail is lighter than a one with a tail, the flying wing would have less weight than a standard UAV configuration. However, the absence of the tail causes two main problems – the wing has to achieve its own stability and there is also no place for the elevators and rudders.

In order to overcome the above problems it was decided to place the elevators on the wing itself, as shown in figure 8. Also, it was decided to add winglets to the configuration and place the rudders on them.
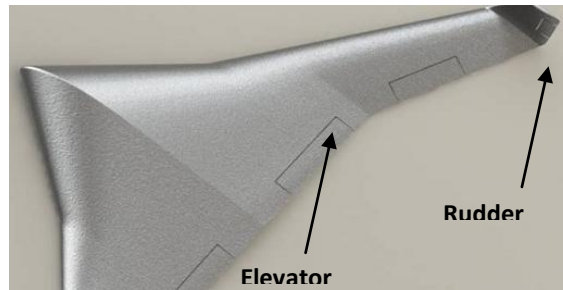
Figure 22

Next, it was necessary to stable the UAV. Stability was achieved by using a reflex profile (figure 23).

Figure 23

As shown in figure 23, the curve of the reflex profile twists upwards at the trailing edge. When the UAV has a positive AOA, the twist of the reflex profile causes a negative moment which counteracts to the AOA and stabilizes the UAV.

Several profiles were compared:

profile	Max t/c	picture
EPPLER E340	13.70%	
EPPLER E334	11.90%	
S5010	9.80%	
NACA M6	12%	
HS520	8.84%	
HS522	8.67%	

Table 9

All six profiles were analyzed with Xfoil program for Reynolds number of 300,000 which is the Reynolds number the UAV is planned to fly in. The following graphs were received:

Figure 24 shows the drag coefficient Vs. the AOA. It can be seen that EPPLER E340 and EPPLER E334 have the lowest drag coefficient for high and that for low AOA the drag coefficients of all profiles are approximately similar.
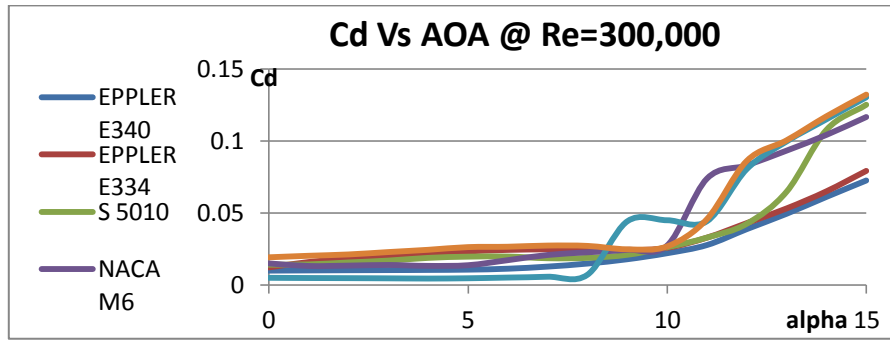
Figure 24

Figure 25 shows the moment coefficient Vs. the AOA. In order to reach stable UAV, C_m must be negative. It can be seen that EPPLER E334 has large negative moment coefficient. Moreover, all other profiles have negligible C_m.
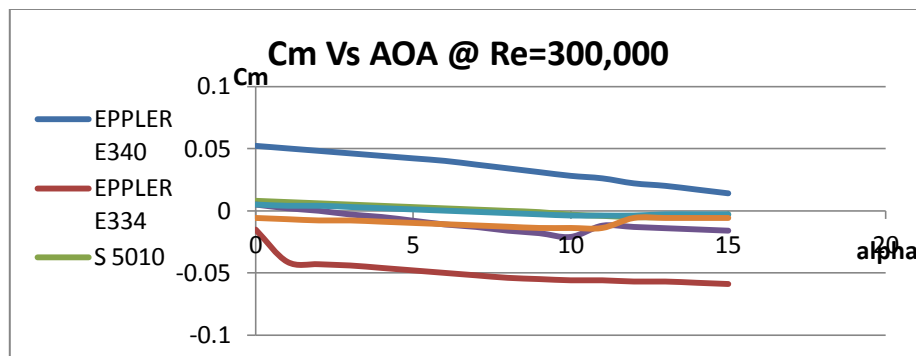

Figure 25

Figure 26 shows the lift coefficient Vs. the AOA. It can be seen that EPPLER E334 has highest lift coefficient and relatively high stall angle.
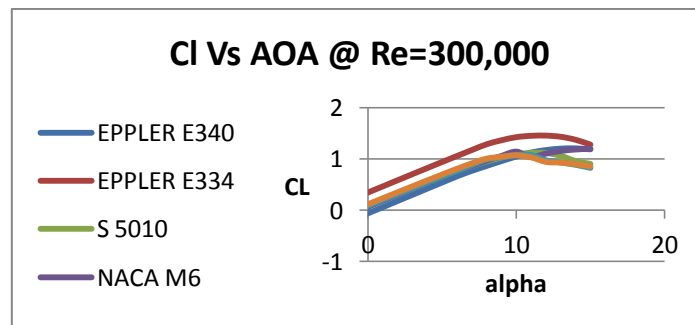

Figure 26

After summarizing all the results, it was decided to use the EPPLER E334 profile especially due to its large thickness and high lift-to-drag ratio. Furthermore, the EPPLER E334 has low drag coefficient, the highest lift coefficient, a relatively high stall angle and a negative moment coefficient.

VI.   PERFORMANCE

In order to examine the aircraft performances, several analyses were carried out.

First, a 3D model was designed using the selected airfoil and the program SolidWorks (27).

Figure 27

A CFD analysis was carried out on the UAV, using the CFD option of the SolidWorks program
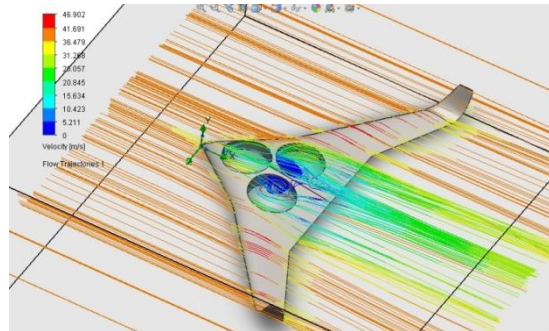

Figure 28

The results showed reasonable flow on the model, and turbulence flow on the cavities

After examining the CFD analysis results, it was concluded, as estimated during the preliminary design, that the cavities of the aircraft led to turbulence and therefore, great loses in performances. The option of closing the cavities was then investigated.
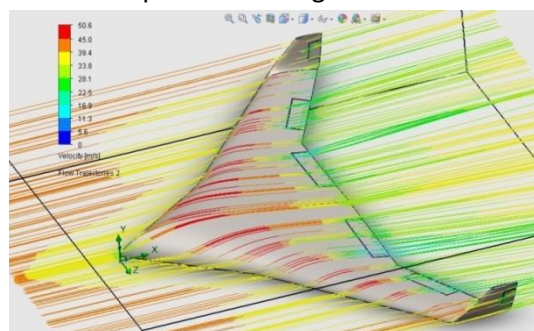

Figure 29

The CFD analysis on the cavity-closed structure showed no turbulence and a satisfying continuous flow.

These results led to the decision of closing the cavities on the structure by some sort of closing mechanism which was determined in the second semester.

After deciding to close the cavities, a numerical analysis of the preliminary performance was carried out using a cavity-closed structure model.

UAV data:

Model top surface-$S = 0.918m^2$
Wing span-$b = 1.77m$
Weight- $W = 9.92lb = 4.5Kg$
Zero-lift drag coefficient-$C_{D_0} = 0.006$
Zero AOA lift coefficient-$C_{L_0} = 0.35$
Lift curve slope-$C_{L_\alpha} = 6.76\frac{1}{rad}$
Stalling AOA-$\alpha_{st} = 11.5^o$

Using a Matlab code, we were able to achieve the drag, power and aerodynamic efficiency diagrams at different cruise velocities of the aircraft:

Figure 30 presents the aircraft aerodynamic efficiency at different cruise velocities.
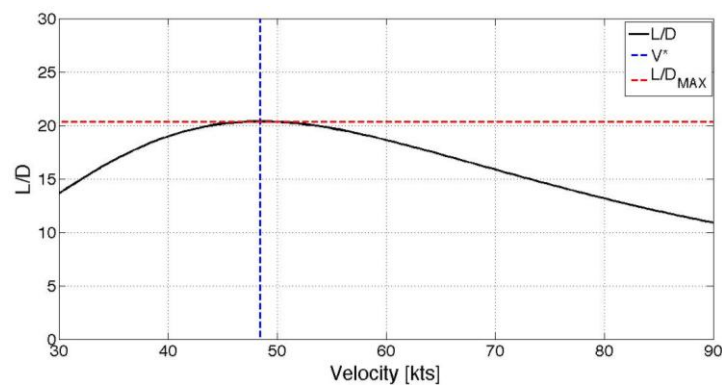

Figure 30

Shown in figure 30 is the calculated $\frac{L}{D}$ at different velocities. As mentioned before, the maximum of the curve is achieved at the speed for minimum drag (V^*), and its value ≈ 20.

Figure 31 presents the aircraft drag at different cruise velocities.

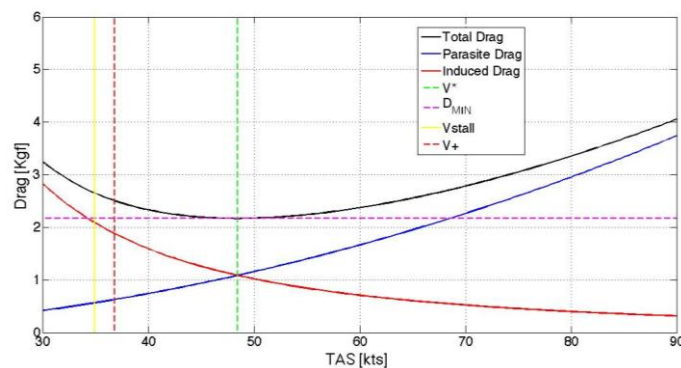**Figure 31**

When examining the graph of the drag above, it was concluded that drag values between $V = 40 - 60\ knots$ is very similar, and this is the range of velocities that at which the aircraft will be the affected by the drag.

The required power at different cruise velocities is presented in figure 32.
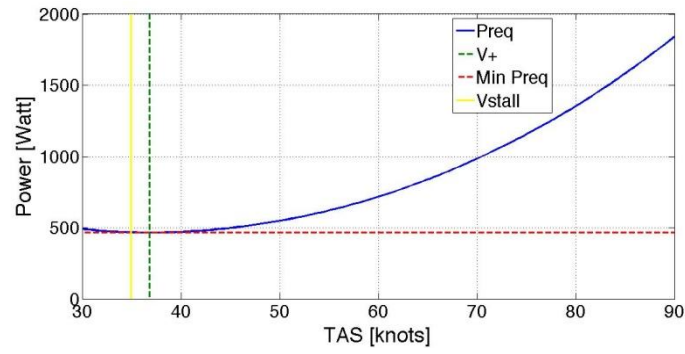
Figure 32

Figure 32 presents the required power for overcoming the drag. When choosing the cruise velocity for the aircraft, this graph is the most important due to the fact that the lower the required power will be during the cruise, the lower the weight of the engines' batteries will be to ensure the endurance needed.

The previous calculations showed that cruise velocity for minimum required power was $V^+ = 36.8$kts but when observing the results, higher velocity was chosen due to the small difference between the calculated velocity V^+ and the stalling velocity $V_{stall} \approx 35kts$.

The cruising velocity was than chosen to be $\approx V^* \approx 48knots$, the required power was calculated- $P_{req} \approx 530Watts$.

Endurance performances:

The batteries for the vertical flight were chosen to work for 2 minutes during the take-off and the landing (each part- 2 minutes) , a reasonable time for the vertical motors to lift the UAV to a minimum height in which the horizontal motor will start working and complete the take-off, and a good time for landing due to fact that less thrust is needed during the landing.

 The batteries for the horizontal flight were chosen to work for 20 minutes and supply a maximum value of 700 Watts (take-off) to the engine at all times. After examining the results from the numerical analysis, it was concluded that the batteries can achieve this endurance and more, due to the lower power that was required during the cruise.
Horizontal endurance – 4 minutes.
Vertical endurance $\approx$ 20 minutes.

Range performances:

Vertical range $-$ $R = V_{cruise} \cdot t_{endurence} = 30Km = 18.64 \ miles$.

Maneuvering performances – V-n diagram:

Maximum load factor was assumed to be $- n_{max} \approx 3.8$
Corner Speed- speed of turns $-$ $V_A = 67.1kts$
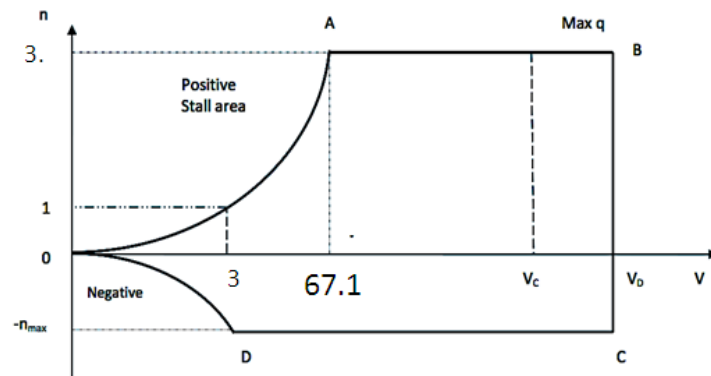Minimum turn radius $- R_{min} = 33m$; V_A

Figure 33

VII.   CAVITY CLOSING MECHANISM

To close the cavities, few options were considered.
The mechanism thickness sholud be minimized in order to avoid conflict with propellers, motor mount and other inner components (figure 34).
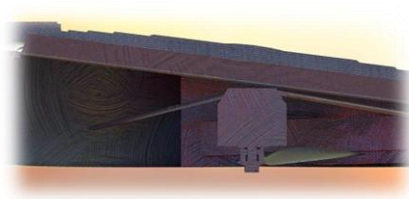

Figure 34

1.   Shutters mechanism

The first mechanism that was investigated was the shutters mechanism, which is a simple mechanism, used in houses.

The shutters mechanism is comprised of a ring to which the shutters are connected with poles. The end of each pole is bended and connected to a wire that rounds the ring from the outside.
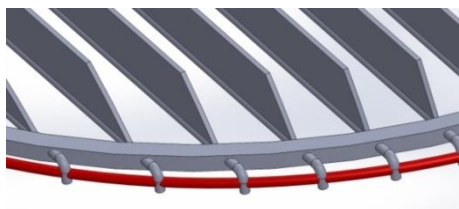

Figure 35

The designed mechanism is presented in figure 36. The inner diameter of the ring is 10 inches which is the diameter of the vertical propeller that was chosen. The outer diameter of the ring is 10.4 inches and the ring's thickness is 5 mm. the shutter's height is 13 mm each and their thickness is 1 mm each. When the shutters are opened, the total height of the mechanism is about 10 mm. the cable's diameter is 2 mm.
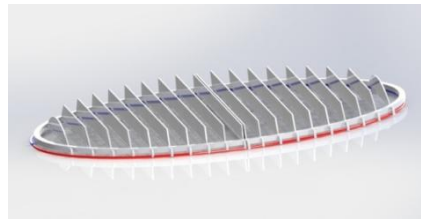

Figure 36a

Figure 36b presents the mechanism closing process. On the top right corner is the fully opened mechanism wile on the bottom is the fully closed mechanism. On the top left corner is the half closed mechanism.
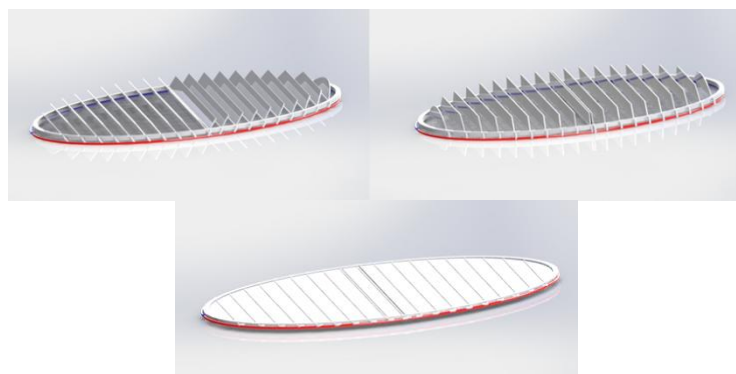

Figure 36b

A study of the shutters mechanism has raised several advantages. The first and most crucial is the small outer diameter of the ring which complies with the maximal diameter allowed under the UAV's limitations. Another advantage is the simplicity of the mechanism as well as its low height in closed configuration. However, during vertical take-off and landing the opened shutters may interrupt the flow and affect the UAV's performance.

2. **Iris mechanism**

Another mechanism we investigated was the Iris mechanism which is a simple shutter, used mainly in cameras, and enables to close a round hole with ease.

The Iris is comprised of two rings mounted on each other, one stationary and one that can rotate. Between the rings are segments that open and close with the rotation of the top ring.
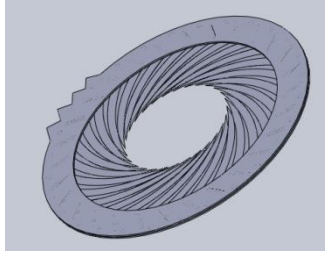
Figure 37

The outer diameter is 13 inches while the inner diameter is 10 inches which is the diameter of the propeller that was chosen. The thickness of the top and base ring is 2mm. In total, there are 28 Segments positioned with a small angle of 5 degrees. The thickness of each segment is 0.2mm. When the iris opens 5 segments are overlapping which brings the total thickness to 5mm.

After studying the Iris mechanism, several advantages were found. The first was that it does not impair the air flow when the hole is fully opened. Another advantage is the simple design which can be operated easily with a small servo.
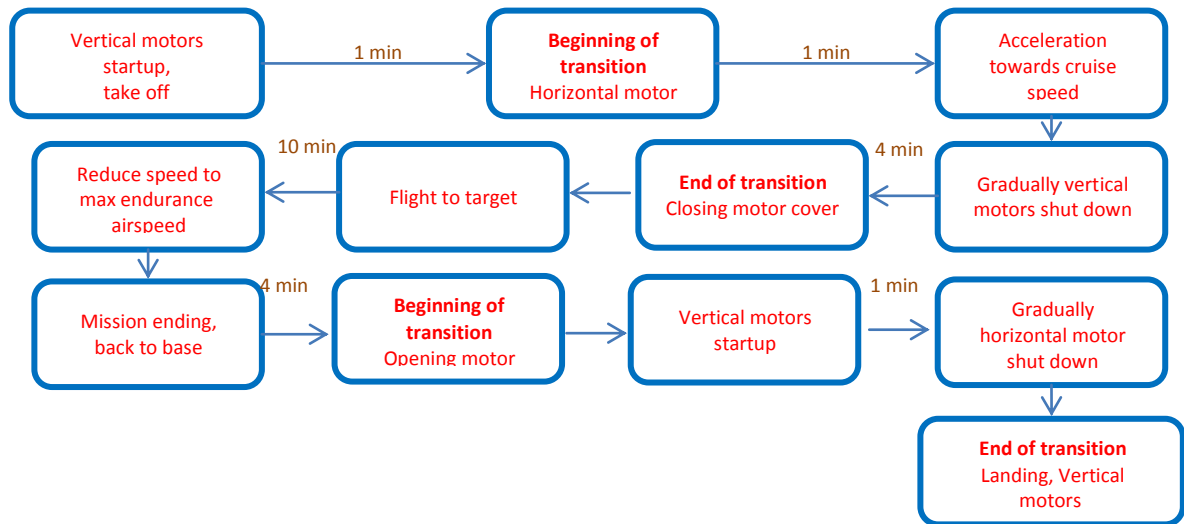
On the other hand, the UAV has limited space and the Iris mechanism requires a diameter larger than the one allowed. Reduction of the outer diameter is dependent of additional segments which will cause friction and inability to open or close the system. Furthermore, since the curved design of the UAV does not comply with the contour of the Iris mechanism, craters will appear in the body and will affect the UAV's performance.

The closing mechanism must have a minimal outer diameter in order to fit into the UAV. Furthermore, the thickness of the mechanism must be as thin as possible since the UAV has limited space in it. Due to these considerations, the chosen mechanism was the shutters which can be installed on top of the UAV rather than in it.

VIII.   CONTROL SYSTEM

Due to the unique design of the UAV, it was decided to use two different control systems: A tri-rotor system to control the ascent and descent altitude and a more common control system to control the level flight.

Figure 50 describes the flight pattern for the UAV, showing approximated times for each step. The pattern shows that at the beginning only the vertical motors are started and that after take-off the horizontal motor is started. Moreover, once the cruise speed has been reached, the vertical motors shut down. The opposite transition takes place at the end of the flight when the vertical motors shut down after landing.

Vertical motors startup, take off	→ 1 min →	**Beginning of transition** Horizontal motor	→ 1 min →	Acceleration towards cruise speed

Reduce speed to max endurance airspeed	← 10 min ←	Flight to target	←	**End of transition** Closing motor cover	← 4 min ←	Gradually vertical motors shut down

Mission ending, back to base	→ 4 min →	**Beginning of transition** Opening motor	→	Vertical motors startup	→ 1 min →	Gradually horizontal motor shut down

End of transition Landing, Vertical motors

IX.   EXPERIMENTS

1. Propeller Selection Test

In order to verify motor and propeller selection, a thrust test has been done.

Figure 38 shows the test setup: the motor and propeller connected to a weight that represents the UAV approximate weight. On the left, the chosen LiPo battery can be seen and on the right, the voltmeter is positioned. At the bottom of the picture, the RPM measurement device can be seen.
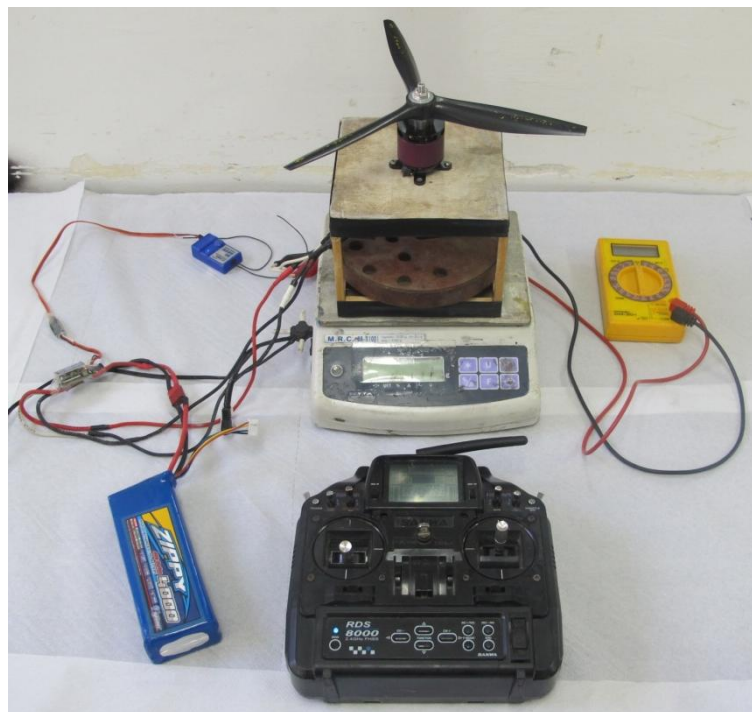

Figure 38

As shown in figure 39 the test included several propellers, some of 2-blades and some of 3-blades.

Figure 39

Table 10 presents the thrust test results. It can be seen that the selection of motor and propeller is satisfying. Though comparing to the prediction less thrust was received, the results were within the required limits of more than 1.5Kg.

Propeller [Diameter X Pitch]	Throttle [%]	Thrust [Kg]
APC 9X3.8	50	
	75	0.9
	100	1.05
APC 9X7.5	50	0.5
	75	1.05
	100	1.09
APC 10X4.7	50	0.77
	75	1.55
	100	1.59

Table 10

The errors during the test mainly resulted from the structure of the test mount. The torque produced by the motor was too strong for the mount structure which had a yaw tendency. In order to correct it, it was necessary to hand held the structure which distributed to the accuracy of the digital weight.

## 2. Configuration Wind Tunnel Test

A wind tunnel test was carried out in the Aerospace faculty wind tunnel.
The main purposes of the wind tunnel were:

- Verifying the predicted performances.
- Examining the option of leaving some of the cavities of the structures.
- Investigating the performances when leaving the cavities.
- Comparing rudders and splitter ailerons for yaw.
- Finding the aerodynamic center.

The chosen scale for the model was 1:2.5 due to the wind tunnel dimensions of 1x1 [m] and maximum blockage percentage of 4%.

A modification has to be done in the model in order to connect it properly to the mount of the tunnel. A cylindrical hole was created from the mid-fuselage backwards and small 'hill'
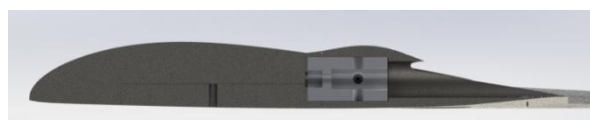
was created above its center. The addition is presented in the following captures from SolidWorks:
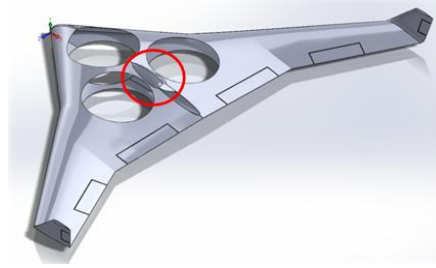

Figure 40

The wind tunnel model was manufactured by rapid prototyping (3D print). The adapter and wing connection plate were manufactured by milling of aluminum. Due to the dimensions of the Objet260 printer, which are 260x260mm, it was necessary to split the fuselage into 4 parts: front, main, right and left wing.

Reynolds number during real flight- $2 \cdot 10^5 < Re < 3 \cdot 10^5$. In order to keep the Reynolds number in this range, the air speed of tunnel has to be -45 $\frac{m}{s} < V < 67 \frac{m}{s}$.

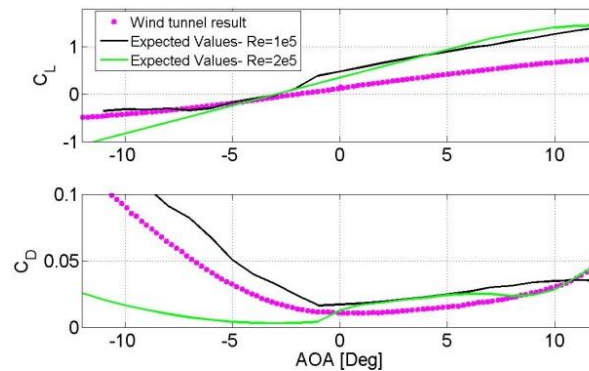**Figure 41 presents the calibration run for$V = 35 \frac{m}{s}$.**

Figure 41

The first run was at tunnel speed- $V = 35 \frac{m}{s}$and different values of AOA. Vibrations on the model were noticed at $\alpha \approx \pm12^O$ as expected. The lift and drag coefficients did not match the expected values of the airfoil at $Re = 2 \cdot 10^5$. When comparing the results to airfoil expected data at $Re = 1 \cdot 10^5$, better match was achieved.

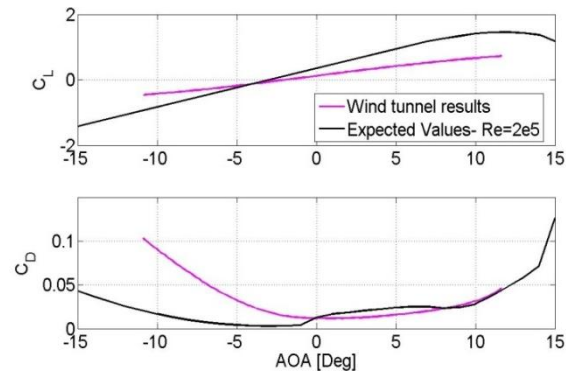**Figure 42 presents the calibration run for$V = 45 \frac{m}{s}$.**

Figure 42

When examining the lift and drag coefficient results at tunnel speed of $45\frac{m}{s}$, there is a good match to the expected values of the airfoil at $Re = 2 \cdot 10^5$.
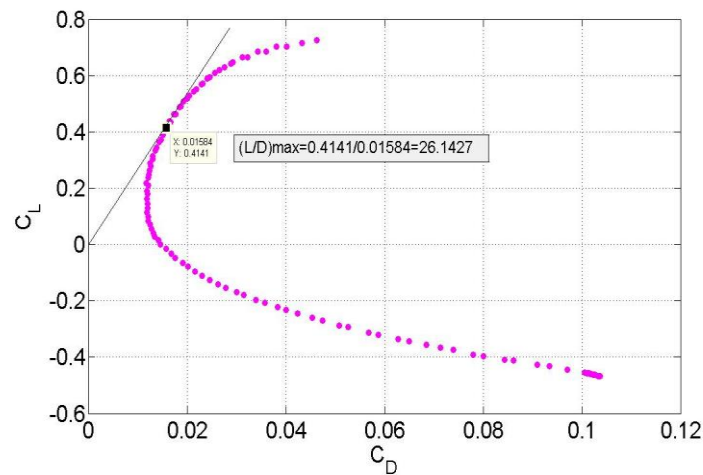

Figure 43

The maximum of the aerodynamic efficiency from the test was 26.14, which was higher than expected.

When comparing the calibration run at $V = 45\frac{m}{s}$ to the expected data, a good match was achieved. The wind tunnel speed was set to $45\frac{m}{s}$ due to the risks to the structure when testing with higher speed. Also, the range of AOA was chosen to be $-10^O < \alpha < 10^O$.

After choosing the speed of the tunnel and the range of AOA, two options for better yaw moment were investigated:

1. Rudders
2. Splitter ailerons

In order to compare the two options, the aerodynamic coefficients were examined (figure 44).
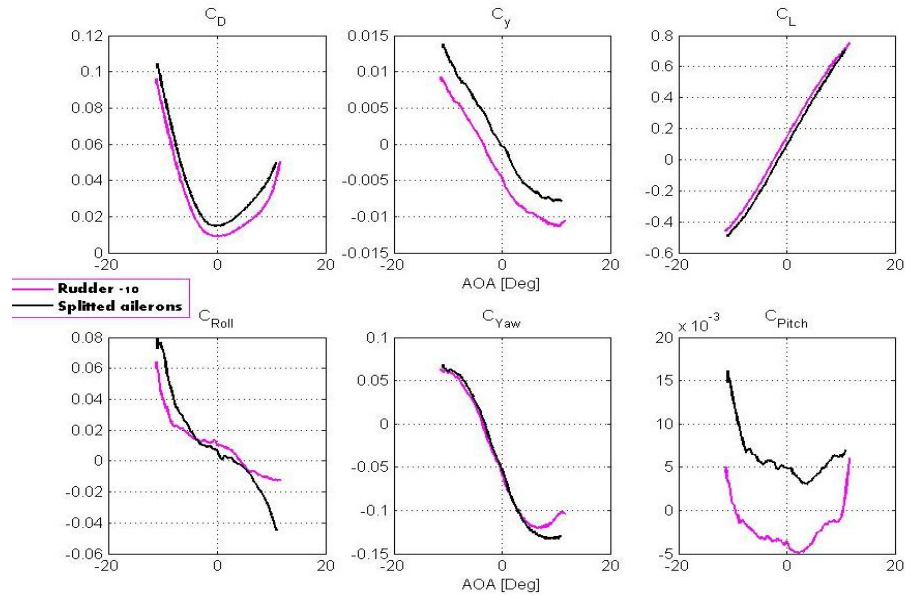
Figure 44

Due to the similar yaw moment coefficient that was achieved using the two options, and the similarity on roll and pitch moments as well, the decision was made using the comparison of the forces coefficients.

When using the rudder for yaw -lower drag, higher lift and lower side force were achieved. The results led to the decision to use rudders for better yaw moment during the actual flight.

Due to the complication of the cavity closing mechanism, the weight of it, and the control problem when designing it, the option of leaving some of the cavities open was investigated.

First, the aerodynamics of the configurations were examined to determine whether the options are possible and then, a performance analysis was carried out to investigate the performance loses.

Five configurations were investigated:

1- All shutters closed
2- Two bottom back shutters open
3- All bottom shutters open
4- Only upper front shutter closed
5- All shutters open

The aerodynamic coefficients of the configurations were compared (figure 45).
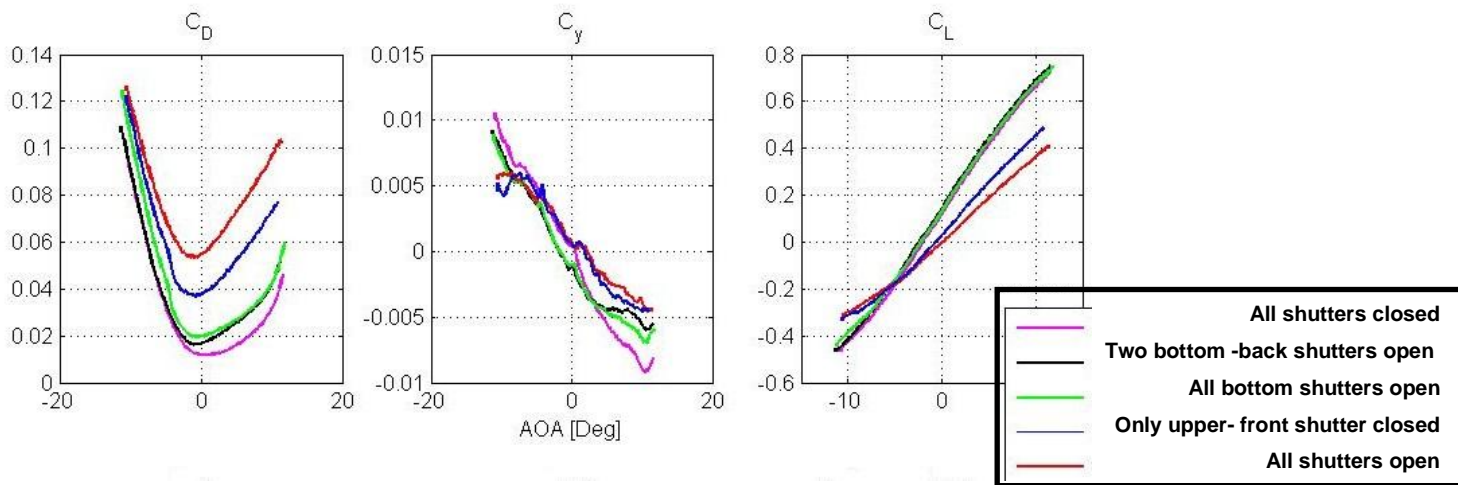
Figure 45

When examining the aerodynamic coefficients differences between the configurations, two main conclusions were achieved from the results:

1- The first three configurations have had similar results.
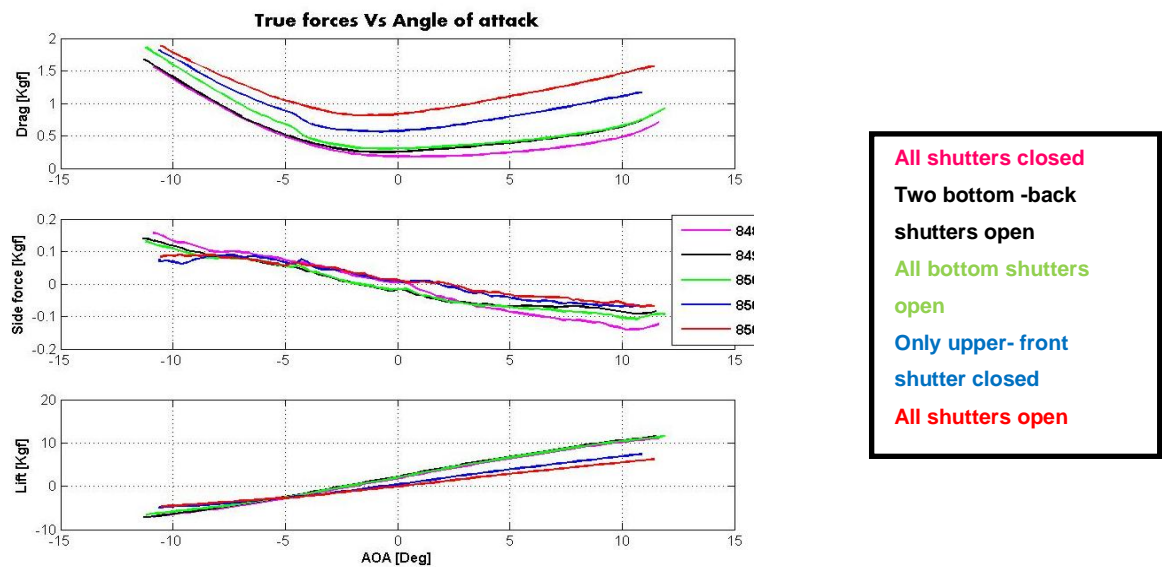2- When fewer cavities are closed, the drag increases.

Figure 46

When examining the true forces on the model (figure 46), the results led to rule out the two last options, due to significantly lower lift and higher drag comparing to the first three options.

It was then decided to rule out the 2nd option of two bottom-back shutters opened due to the similarity of it to the option of all bottom shutters opened, and that the purpose was to leave as many cavities opened as possible.

The following comparisons were between two options- the closed configuration and the option of bottom shutters open.

Yaw comparison (figure 47):
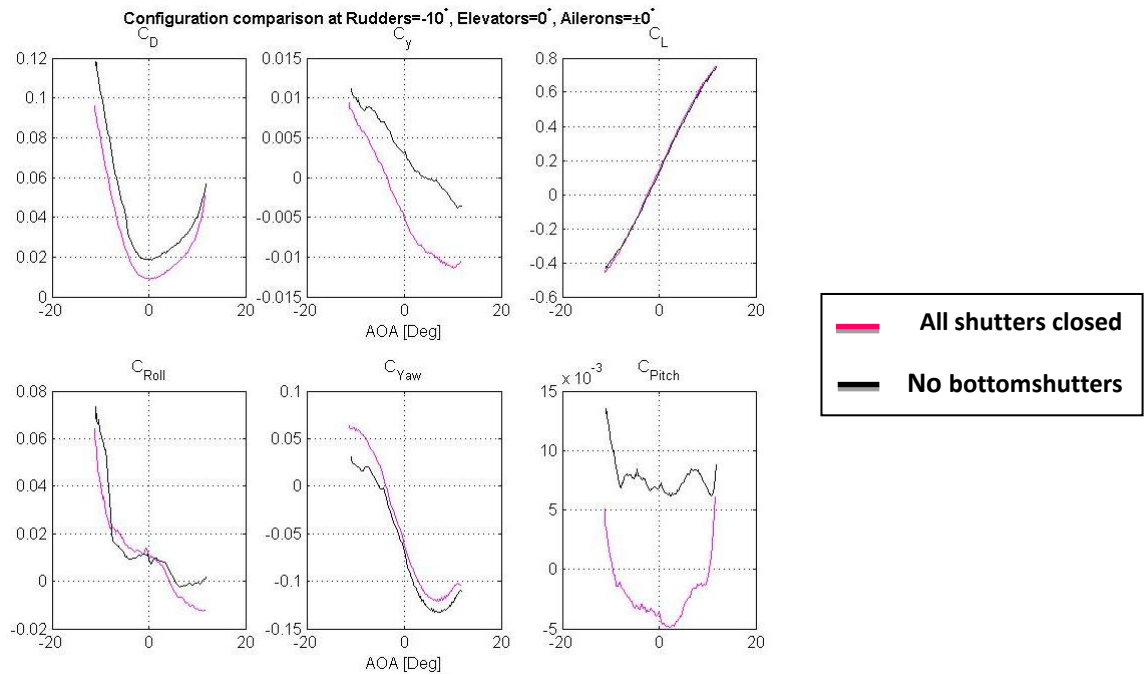
Figure 47

It was noticed that better yaw moment is achieved with closed configuration although the difference was minor. The drag has increased when using the opened bottom covers configuration, as expected. Also, side force has increased significantly. The lift coefficient was very similar, a result that was not expected.

On the pitch and roll experiment, the results were similar. A greater drag was measured on the opened- bottom configuration, a very similar lift and side force were achieved on both configurations.

Figure 48

Figure 49

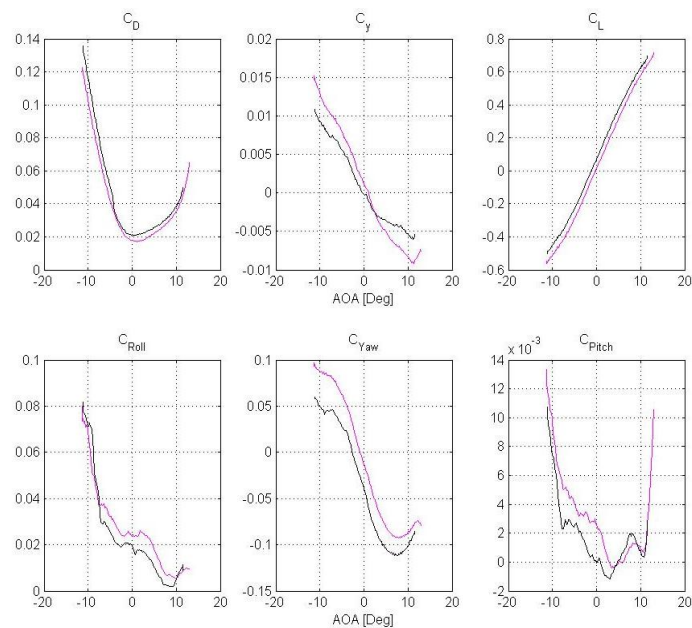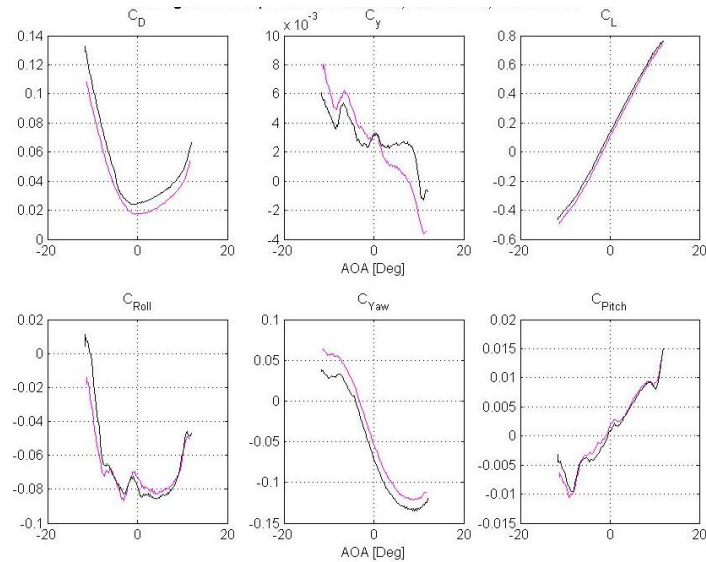When examining the moments coefficients- on the pitch comparison- the opened configuration had higher moment values, while on the roll comparison- the results were very similar.

The option of no shutters mechanism on the bottom surface of the UAV was aerodynamically examined for level flight, roll, pitch and yaw maneuvers and was concluded to be reasonably possible.

		Preliminary analysis results	Experimental Results- All Shutters Closed	Experimental Results- Bottom Shutters Open
Stalling Speed	[Kts]	34.95	27.55	28.02

Table 11

The stalling speed of the UAV (table 11), according to the wind tunnel test, was lower than expected, and was 78% of the expected value. Also, when removing the bottom closing mechanism, the stalling speed was slightly higher (by 1.07%). Overall, the test results were in good match to the theory, and there was no significant change between the configurations.
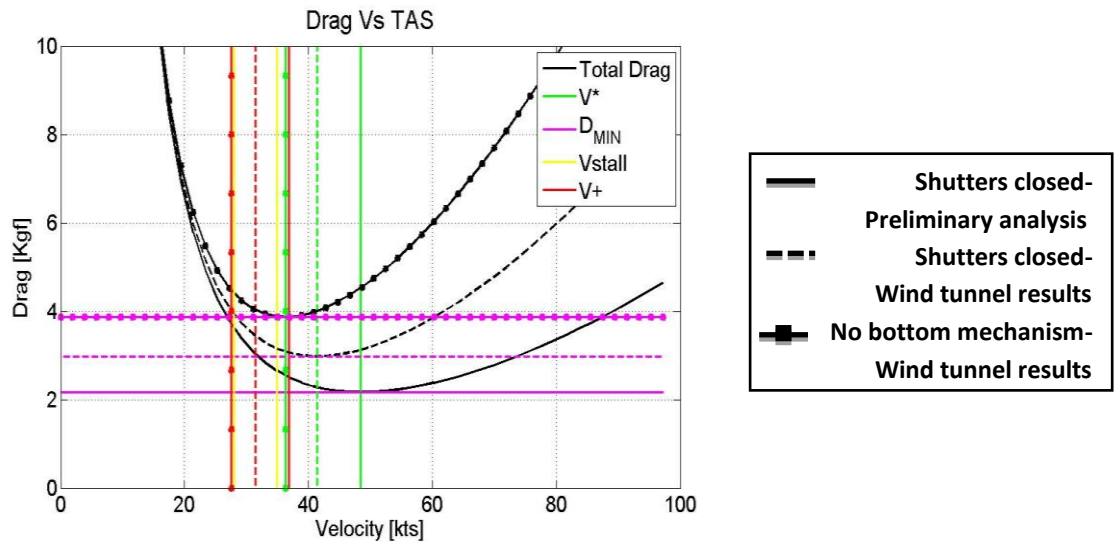
Figure 50

Figure 50 presents the drag on the UAV vs. the flight speed.

The drag on the closed configuration was higher than expected. Also, when removing the bottom closing mechanism the drag rises. Moreover, the velocity of the minimum drag value V^* was lower than expected and decreased when removing the bottom closing mechanism.

Figure 50 shows that the range of velocities in which low drag values are achieved, was smaller with the bottom mechanism removed.

		Preliminary analysis results	Experimental Results- All Shutters Closed	Experimental Results- Bottom Shutters Open
Minimum Drag	[Kgf]	2.17	2.97	3.86
At Speed Of	[Kts]	48.46	41.35	36.3

Table 12

Closed configuration drag was 36.8% higher than expected, and at a speed of 41.36 knots, which was 85.3% of the expected value. Overall, when considering the changes that were made to the UAV airfoil due to the wind tunnel limits, there was a good match between the expected values from the theory and the wind tunnel test results.
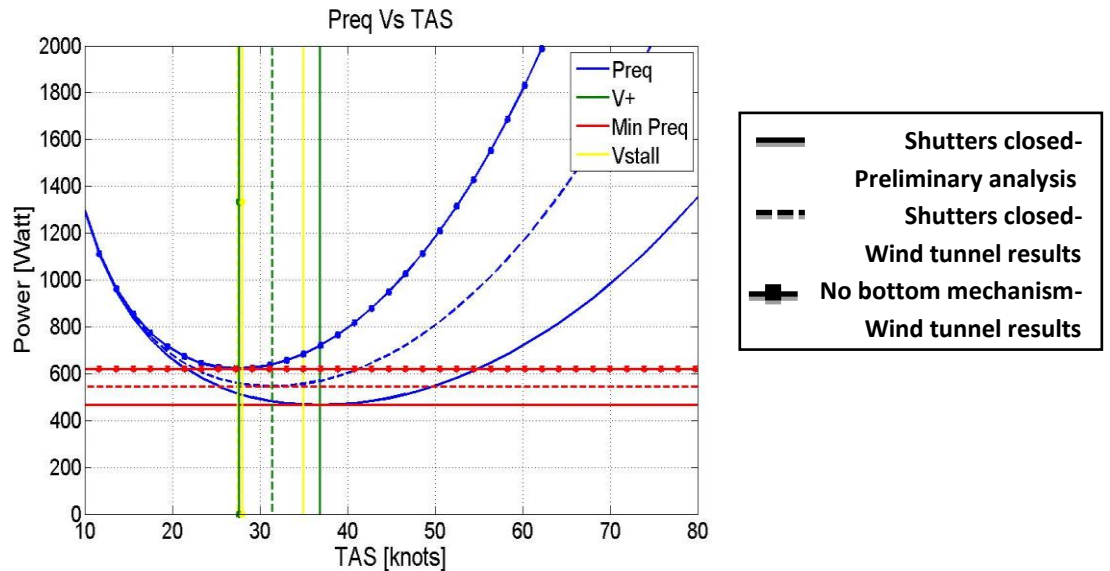
Figure 51

In order to determine whether the horizontal engine will be able to overcome the drag of the UAV, a power comparison was carried out (figure 51). The results showed higher values of required power at lower velocities V^+ for the closed configuration than expected.

Another important result was the fact that the velocity for minimum required power, when investigating the configuration with no bottom closing mechanism, was lower than the stalling velocity. This observation proved the decision to cruise at a higher velocity, which was made in the preliminary performance analysis.

		Preliminary analysis results	Experimental Results- All Shutters Closed	Experimental Results- Bottom Shutters Open	Chosen cruising velocity
Minimum required power	[Watts]	465.2	545.2	621	651.1
At Speed Of	[Kts]	36.8	31.42	27.6	33

Table 13

As seen in table 13, the required power for closed configuration was higher by 17.2% than expected, which was a good match to the expected value. When examining the configuration with no bottom closing mechanism, the minimum required power was 621 watts which was 13.8% higher than the closed configuration.

When choosing the engine for the horizontal flight, it was determined that the engine could supply approximately 700 watts through the entire flight. Choosing a higher cruise velocity of 33 knots led to higher required power value of 651.1 watts, which was lower than the horizontal engine limit. **Overall, it was concluded that the engine will be able to overcome the drag of the UAV with or without the bottom closing mechanism.**

Due to the fact that the required power has not exceeded the expected power supply of the engine, the endurance has not changed.

When combining the vertical and horizontal flight, the endurance will be approximately 24 minutes.

When investigating the range of the UAV, the results can vary when choosing different cruise velocities. As can be seen in table 14, the closed configuration range was approximately 17% lower than expected.

		Preliminary analysis results	Experimental Results- All Shutters Closed	Experimental Results- Bottom Shutters Open
Maximum	[Km]	30	24.7	20.4
range	[Miles]	18.64	15.35	12.7
At Speed Of	[Kts]	48	40	33

Table 14

The range of the UAV was affected by removing the bottom closing mechanism and was approximately 15% lower than the closed configuration, a value of 4Km or 2.5 miles.

X.   SUMMARY

The costumer's requirements defined the future product as a small portable UAV, carried and operated by one unskilled person with endurance of 30 and real time video photography capabilities.

Starting with market survey, it was found that a mini-UAV category is suitable for the requirements, including 'toys' that influenced the concept. Due to the survey, it was chosen to combine between a quad-rotor and a flying wing.

This innovatory concept required three vertical motors and one horizontal motor.

As planned, the motors were located inside the wing itself which required a closing mechanism for the cavities of the motors.

After conceptual design was completed, the components and systems were chosen.For propulsion, it was decided to use electric motors which are more quiet and easy to operate. The propellers were chosen to match the motors after considering two and three blades. The choices were verified using theoretical calculation as well as a thrust test. Furthermore, batteries were chosen in order to fit the endurance requirement and weight limitation. The payload was chosen based on the performance and weight.

After all the components and systems were chosen, a calculation of weight and balance was made and the systems were arranged inside the fuselage.

Also, the aerodynamic was analyzed, including airfoil selection, winglets configuration and performance analysis.

The next stage was conceptual and detailed design of the wing structure, choosing materials and creating a 3D model. Moreover, cavity closing system was planned in order to close the cavities of the vertical motors.

The final stage was designing and manufacturing a wind tunnel model and conduction of a wing tunnel test. The test results were analyzed and compared to the performance analysis.

XI. REFERENCES

1. John B. Brandt and Michael S. Selig†, **Propeller Performance Data at Low Reynolds Numbers**, University of Illinois, USA, <u>AIAA</u>

2. J. Cristofol, Y. Hertienne, M. Lafleur, B. Verguet and S. Vitu, **Tri-rotors UAV Stabilization for Vertical Takeoff and Hovering**, Ecole Centrale d'Electronique, Paris, France

3. Dr Stephen D. Prior, Dr Mehmet Karamanoglu, SiddharthOdedra, Mehmet Ali Erbil and Tom Foran, **Development of a Co-Axial Tri-Rotor UAV**, Middlesex University, London, England.

4. S.D. Prior, S-T. Shen, M. Karamanoglu, S. Odedra, M. Erbil, C. Barlow and D. Lewis1, **The Future of Battlefield Micro Air Vehicle Systems**, Middlesex University, London, England.

5. Jean Koster, Scott Balaban, Andrew Brewer, Chelsea Goodman, Derek Hillery, Cody Humbargar, Mark Johnson, Mikhail Kosyan, Derek Nasso, Julie Price, Eric Serani, Alec Velazco, Tom Wiley, and Richard Zhao, **Hyperion Flying Wing Aircraft Technology**, University of Colorado, USA.

6. PRASETYO EDI, NUKMAN YUSOFF and AZNIJAR AHMAD YAZID, **Airfoil Design for Flying Wing UAV (Unmanned Aerial Vehicle)**, University of Malaya, Kuala Lumpur, MALAYSIA.

7. Kai Lehmkuehler, KC Wong and Dries Verstraete**, DESIGN AND TEST OF A UAV BLENDED WING BODY CONFIGURATION**, The University of Sydney, Australia.

8. NavabalachandranJayabalan , Low Jun Horng, G. Leng, **Reverse Engineering and Aerodynamic Analysis of a Flying Wing UAV**, National University of Singapore, Singapore.